

Thermodynamics of the fully frustrated quantum Josephson-junction array: A hybrid Monte Carlo study

J. Mikalopas, M. Jarrell, F. J. Pinski, and Woonki Chung
Department of Physics, University of Cincinnati, Cincinnati, Ohio 45221-0011

M. A. Novotny
Supercomputer Computations Research Institute, Florida State University, Tallahassee, Florida 32306-4052
(Received 7 April 1994)

We use a hybrid Monte Carlo algorithm to simulate the thermodynamic properties of a two-dimensional periodic array of fully frustrated quantum Josephson junctions. We find a variety of metastable configurations that correspond to spatial domain boundaries that are also present in classical arrays. In previous work, due to long temporal correlations between configurations in diffusive Monte Carlo algorithms, such metastable states were interpreted as evidence for a quantum-induced low-temperature first-order transition.

In the literature, there exist many model calculations of granular superconductors coupled by Josephson tunnel barriers. Early, it was implied¹⁻³ that the electrostatic charging energy associated with ultrasmall metal grains could have a profound effect on the superconducting properties of the aggregate. This electrostatic charging energy is due to the finite capacitance of the small metal grains and is therefore associated with the transfer of electrons between grains. For systems in which the conductors are small or mesoscopic, the effect of this electrostatic energy may be large.

Perhaps the most dramatic such effect was reported by Jacobs and co-workers⁴⁻⁶ who detected a first-order transition at low temperatures in their simulations of quantum Josephson-junction arrays. They claim that this transition was one from the usual superconducting state to a novel zero-resistance coherent state dominated by zero-point quantum fluctuations. They refer to this as a "quantum-induced transition" (QUIT). This effect, which was found using diffusive Monte Carlo calculations, was seen by a maximum in the specific heat and a nonmonotonic behavior in the helicity modulus as the temperature went through T_{QUIT} . They reported that the QUIT was far more pronounced in the case when a transverse magnetic field was applied to obtain a fully frustrated array.

In this paper, we report a series of calculations that provide evidence that the QUIT, that they observed, results from spatial domain boundaries which are also observed in classical arrays. We attribute the previous evidence for the QUIT to limitations of the diffusive Monte Carlo algorithm employed in the work by Jacobs and co-workers. Subsequent to their studies, substantial advances have been made in Monte Carlo algorithms. In our simulations, we employ a hybrid Monte Carlo algorithm⁷⁻⁹ in which the field variables are allowed to evolve *globally* under a set of Hamilton-Jacobi equations. By such a sampling procedure, the hybrid Monte Carlo removes the strong correlations that can exist between consecutive configurations in a diffusive Monte Carlo algorithm. Using this algorithm, we do not find evidence for a quantum-induced transition.

Following Jacobs and co-workers, we model a granular material with ultrasmall grains with a periodic array of Jo-

sephson junctions with finite coefficients of capacity. The topology of the array is taken to be a two-dimensional square lattice with periodic boundary conditions. The Josephson junctions have an identical temperature-independent coupling constant and only the diagonal contribution of the capacitance matrix is included in the electrostatic charging energy.

The corresponding Hamiltonian has the form

$$H = \sum_{\langle i,j \rangle} \epsilon_C n_{i,j}^2 + \epsilon_J \{ 2 - \cos(\phi_{i+1,j} - \phi_{i,j} - \psi_{i,i+1}) - \cos(\phi_{i,j+1} - \phi_{i,j} - \psi_{j,j+1}) \}. \quad (1)$$

The sum is over the neighboring sites, indexed by an i and j , of a two-dimensional square lattice. The $\phi_{i,j}$ are the phase of the Ginzburg-Landau superconducting order parameter associated with each grain and the $n_{i,j}$ measure the number of Cooper pairs transferred between grains. The Josephson coupling energy associated with each junction is ϵ_J , and ϵ_C is the electrostatic charging energy associated with each grain. We choose our unit of energy such that $\epsilon_J = 1$. The link integrals $\psi_{i,i+1} = (2\pi/\Phi_0) \int_i^{i+1} \mathbf{A} \cdot d\mathbf{l}$, are proportional to the line integrals of the magnetic vector potential \mathbf{A} between nearest-neighbor sites where Φ_0 is the fundamental quantum of flux. The uniform frustration parameter f , which identifies the number of flux quanta per plaquette, is equal to the sum around an elementary plaquette of the link integrals divided by 2π , that is $2\pi f = \sum_p \psi$. We will restrict ourselves to the fully frustrated case, $f = \frac{1}{2}$. In our simulations, the Landau potential $\mathbf{A} = Bx\hat{y}$ is chosen, with B being the applied external magnetic field.

The thermodynamic properties associated with H are calculated by using a quantum Monte Carlo algorithm. The formalism is based on Feynman's imaginary-time representation of the corresponding quantum partition function $Z = \int D\phi e^{-S\{\phi\}}$. The discretized expression for the action $S\{\phi\}$ is given by Eq. (3.20) of Ref. 6.

In a conventional Monte Carlo procedure, the expectation value of a physical quantity $\langle A \rangle$ is evaluated by generating a sequence of configurations of the scalar fields $\{\phi_m\}$, with

probability $P\{\phi_m\}$. As commonly employed, the sampling of fields $\{\phi_m\}$ is diffusive. New configurations are generated by proposing only local, random changes to the field variables of the present configuration. Strong correlations can exist between consecutive configurations of the field variables in a diffusive Monte Carlo algorithm. For example, the sampling can become trapped in the vicinity of a local minimum of the action and therefore confine the sampling to an overly limited region of phase space.

The hybrid Monte Carlo method^{7,8} was developed to alleviate this problem⁹ while retaining the property of detailed balance. In the hybrid method, a fictitious momentum π is assigned to each of the variables ϕ . The dynamics of this pseudosystem are described by the pseudo-Hamiltonian, $H_p\{\pi(t), \phi(t)\} = \pi^2(t)/2 + S\{\phi(t)\}$, and the corresponding Hamilton-Jacobi equations of motion. We used a Gaussian distribution for the pseudomomenta $\pi(0)$ and approximated the solutions of these equations by using the leapfrog algorithm.¹⁰ A pseudopartition function, $Z_p = \int D\pi \times \int D\phi e^{-\beta H_p\{\pi(t), \phi(t)\}}$, is associated with this pseudo-Hamiltonian. Because the integrand for each of the fictitious momenta is Gaussian, the integral over these fictitious momenta is easily performed to yield $Z_p = (2\pi\mu)^{(V/2)}Z$. Since the pseudopartition function differs from the true partition function by only a multiplicative constant, the expectation values of the physical observables will be identical for both the true and pseudosystem.

We probed several possibilities for the choices of the fictitious time $t = N_t \Delta_t$, the number of pseudo-time-steps N_t , and the size of the pseudo-time-step Δ_t . Because of the errors associated with any numerical integration scheme, the pseudoenergy will begin to deviate from its initial value after some time. The resulting configuration at the end of the Hamilton-Jacobi evolution $\{\phi'_m\}$ is therefore accepted or rejected with the probability $\min(1, e^{\delta H_p})$, where $\delta H_p \equiv H\{\phi'_m\} - H_p\{\phi'_m\}$. Thus in the hybrid method⁸ errors associated with the finite-size Δ_t are only of importance in that they change the acceptance rate of the Monte Carlo configurations, and hence limit the time scale over which a configuration can evolve microcanonically before it has a high probability of being rejected. The pseudo-time-step Δ_t was chosen such that the deviation from energy conservation yielded a Monte Carlo acceptance rate of approximately 95%. Within this constraint, for separate simulations, the number of pseudo-time-steps N_t was varied such that the pseudotime t spanned several orders of magnitude.

First, we summarize some of the results concerning the QUIT reported⁴⁻⁶ by Jacobs and co-workers. Consider one of their simulations, an $N \times N \times N_\tau$ lattice with $N=8$ and $N_\tau=30$ with $\epsilon_J=1.0$, $\epsilon_C=0.3$. Their evidence for the QUIT was a discontinuity in the helicity modulus ΔY , typical of a first-order phase transition. The helicity modulus Y measures the response of the array to a long-wavelength twist along a spatial direction and is directly proportional to the superfluid density. Unlike a reentrant transition, where $Y \rightarrow 0$ as $T \rightarrow 0$, the value of the helicity modulus Y had a finite value as $T \rightarrow 0$. The discontinuity in the helicity modulus ΔY was far more pronounced for the fully frustrated system ($f=\frac{1}{2}$) than for the unfrustrated system ($f=0$). For $f=0$, they found $\Delta Y \approx 0.03$ at $T \approx 0.03$, and for $f=\frac{1}{2}$, $\Delta Y \approx 0.15$ at $T \approx 0.15$.

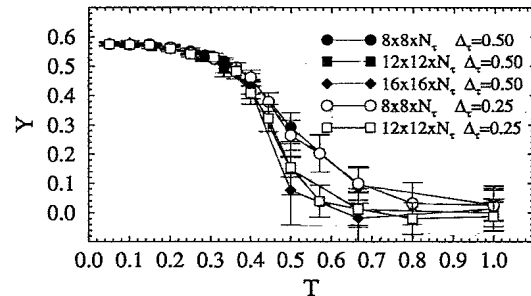


FIG. 1. The helicity modulus Y as a function of T for $f=\frac{1}{2}$ and $\epsilon_C=0.3$ for three spatial lattice sizes ($N=8,12,16$) and values of $\Delta\tau$. Not evident in Y is a discontinuity, at $T < T_c \approx 0.45$, that would indicate a phase transition at low temperatures from the usual superconducting state.

Thus, we concentrated entirely on the system with $f=\frac{1}{2}$. We calculated the helicity modulus using the discretized expression given in Ref. 6. Our principal result is shown in Fig. 1, where we plot the helicity modulus Y for different system sizes and values of $\Delta\tau$. To facilitate comparison, we chose the most commonly used parameters used by Jacobs and co-workers. We find that the maximum slope dY/dT increases with system size, as expected for a superconducting transition. We estimate the superconducting transition temperature, $T_c \approx 0.45$, in agreement with Ref. 6. Not evident in Y is any discontinuity that would indicate a phase transition at low temperatures from the usual superconducting state. In particular for $T < 0.15$, where the QUIT was previously reported, Y is smooth. In addition, we computed values for the internal energy for the same sets of parameters (not shown). Again, not evident is a discontinuity that would indicate a phase transition at low temperatures from the usual superconducting state.

We believe that the discontinuity in the helicity modulus found by Jacobs and co-workers was caused by metastable states that appear very long lived with diffusive Monte Carlo algorithms. The discontinuities are due to their simulations becoming trapped in a local minimum of the action $S\{\phi\}$. We will show that these local minima correspond to metastable configurations that have spatial domain boundaries. These metastable configurations are also observed in classical arrays. A diffusive Monte Carlo algorithm does not readily accommodate the coherent change of phases needed to evolve away from such a minimum.

In order to learn about the transport in the array, we defined the gauge-invariant quantity $\Theta_{i,j}(\tau)$, which is proportional to the supercurrent flowing around the nearest-neighbor plaquette of junctions with lower-left corner i,j . To determine the origins of the QUIT metastability, we set $\epsilon_C=0$ and investigate the fully frustrated ($f=\frac{1}{2}$) two-dimensional classical model. Here also, we encountered metastable configurations. Contributions from these metastable configurations lead to a decrease in the helicity modulus. If the simulation remains trapped in these states, then the helicity modulus would show a fictitious decrease. In a properly ergodic simulation, these metastable configurations are seldomly sampled since they correspond to a relatively large excitation energy.

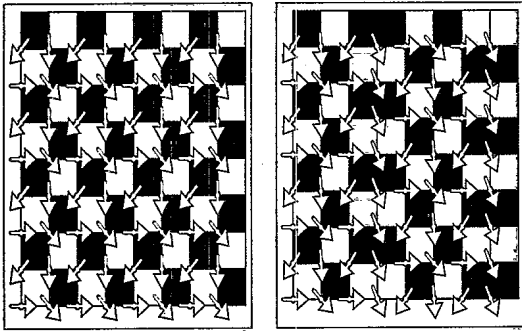


FIG. 2. A low-temperature highly probable equilibrium (left) and a metastable (right) configuration of the fully frustrated ($f = \frac{1}{2}$) classical two-dimensional Josephson-junction array. Shown are the $\phi_{i,j}$ fields and the density plot of the gauge-invariant plaquette current $\Theta_{i,j}$. Note the periodic boundary conditions and the two vertical domain boundaries in the right figure.

One of these metastable configurations found in the classical simulations is shown in Fig. 2 (right side), whereas the appropriate classical ground state is shown on the left. Here the black (white) squares correspond to a clockwise (counterclockwise) current flowing around the plaquette. The magnitude of the plaquette current $\Theta_{i,j}$, is indicated by the grey-scale. The ground state is a black-white chess-board pattern. Comparing the two results, it is clear that the metastable configuration contains domain boundaries characterized by the exchange of the black and white sublattices. In this example, the domain boundaries are separated by four lattice spacings. A diffusive algorithm will not readily evolve away such extended defects since large energy barriers must be overcome.

To determine if similar metastable configurations exist in the quantum model, we considered one of the configurations characteristic of the proposed QUIT state from the original work of Jacobs and co-workers. For this configuration, we found domain boundaries in the spatial plane for each time slice similar to that found in the classical simulation. This is

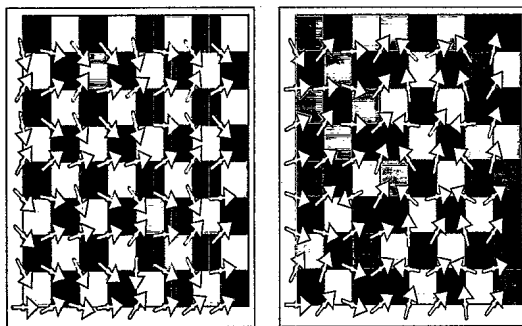


FIG. 3. A representative configuration at $T=0.12$ (left) and the QUIT (right) configuration (from Jacobs and co-workers' simulations) for the fully frustrated ($f = \frac{1}{2}$) quantum two-dimensional Josephson-junction array. The τ -averaged ϕ variables are displayed on top of the density plot of the τ -averaged gauge-invariant quantity $\Theta_{i,j}(\tau)$. Note the periodic boundary conditions.

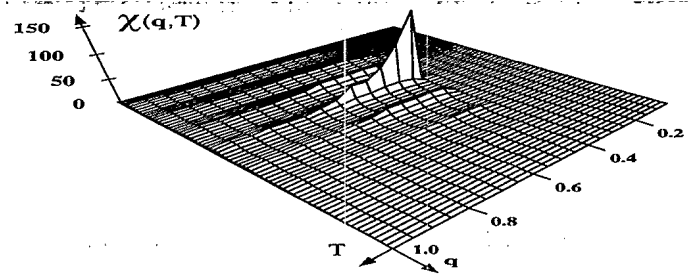


FIG. 4. The average plaquette current susceptibility [defined by Eq. (2)] for $\epsilon_c=0.3$, $f=\frac{1}{2}$, $N=8$, and $\Delta_\tau=0.5$. For these parameters, the critical transition is $T_c \approx 0.45$. The \mathbf{q} vector corresponds to sequential horizontal sections of the Brillouin zone, centered at $\mathbf{k}=(\mathbf{0}, \mathbf{0})$. That is, the q is determined by sweeping q_x and q_y from 0 to 2π , with q_x swept faster. The dominant $\chi(\mathbf{q}, T)$ has $\mathbf{q}=(\pi, \pi)$ corresponding to the emergence of the chess-board pattern shown in Fig. 3 (left), whereas the smaller adjacent peaks correspond to the QUIT configuration Fig. 3 (right).

illustrated in Fig. 3, where we present two imaginary-time-averaged spatial configurations. The right one is representative of the QUIT state. The left, a low-temperature highly probable (LTHP) configuration, is characterized by small fluctuations of a ground-state configuration.

In a LTHP configuration, we find the order of the currents in the spatial planes for each time slice τ to be very similar to that in the ground state of the classical two-dimensional Josephson-junction array. Thus the QUIT state is characterized by the existence of extended defects similar to those found in the classical system.

If we started with a configuration obtained from Jacobs and co-workers that was representative of the QUIT state, then our simulations evolved into the usual superconducting state. We found that our simulations became trapped in various local minima only when the path through phase space was short, i.e., either the number of pseudo-time-steps N_t or the total number of Monte Carlo steps were small. The QUIT state was never robust with respect to an increase in the number of pseudo-time-steps N_t , or an increase in the total number of Monte Carlo steps. Simulations were also performed where the N_t and the Δ_t were chosen randomly from within finite bounds. These also did not get trapped in the QUIT configuration.

Of course, the thermodynamic properties of the system are not characterized by a few configurations such as those discussed above. Therefore, to gain quantitative insight into the effect of these configurations on the thermodynamic properties, we investigated the average plaquette-current susceptibility as shown in Fig. 4. The plaquette-current susceptibility is

$$\begin{aligned} \chi(\mathbf{q}, T) = & \frac{T}{N^2} \sum_{i,j;i',j'} \exp[i\mathbf{q} \cdot (\mathbf{R}_{i,j} - \mathbf{R}_{i',j'})] \\ & \times \int_0^\beta d\tau \int_0^\beta d\tau' [\langle \Theta_{i,j}(\tau) \Theta_{i',j'}(\tau + \tau') \rangle \\ & - \langle \Theta_{i,j}(\tau) \rangle \langle \Theta_{i',j'}(\tau') \rangle]. \end{aligned} \quad (2)$$

Here the different peaks correspond to predominance of certain configurations. For example, the largest peak at the center of the graph corresponds to an ordering in the chess-board pattern illustrated in Fig. 3 (left). As we increase the system size (not shown), this peak appears to scale with system size, perhaps indicating an Ising-like transition.^{11,12} These results show that in the spatial plane, the ordering of the currents (or phases) is similar to the classical array. The plaquette-current susceptibility peaks at roughly the transition temperature T_c for each system size simulated. The two closest secondary peaks correspond to the metastable configurations similar to that pictured in Fig. 3 (right), and the counterpart of this configuration rotated by $\pi/2$. Unlike the central peak, these do not scale with the system size, and hence are not indicators of low-temperature order. The presence of several peaks reinforces our claim that the hybrid Monte Carlo algorithm samples large, well-separated, regions of phase space.

In this paper, we present results from a quantum Monte Carlo simulation of a two-dimensional periodic array of ultrasmall fully frustrated Josephson junctions. The model includes both the Josephson energy due to the weak coupling of the grains and the electrostatic energy due to the charging of the grains. In our simulations, we employ a hybrid Monte Carlo algorithm which eliminates most of the correlation between consecutive configurations of the field variables. We do not find a previously reported first-order phase transition at low temperatures.

Our results indicate that the behavior of these arrays is qualitatively similar to that of classical arrays. The quantum

effects modify features but do not introduce additional phenomena. In particular, we find a variety of metastable configurations corresponding to spatial domain boundaries that are also present in classical arrays. We attribute the misidentification of the QUIT in previous work to the simulation becoming trapped in metastable states near local minima of the action $S\{\phi\}$. We cannot rule out the possibility that a QUIT occurs at lower temperatures than those simulated by us. However, we conclude that if there is a QUIT, it occurs at a very low temperature ($T_{\text{QUIT}} < 0.05 \epsilon_J$, when $\epsilon_C = 0.3$). Another possibility is that the QUIT state has a correlation length much larger than the lattice sizes studied here or by Jacobs and co-workers, and would only be observed for much larger arrays. The metastable configurations reported by Jacobs and co-workers may be relevant to real systems, since, as we have shown, these metastable configurations result from spatial (not temporal) features, and may be stabilized by lattice defects.

We would like to thank J. V. José, D. Stroud, and P. Suranyi for useful conversations. We would especially like to thank J. E. Gubernatis for helpful conversations concerning the hybrid method. This work was supported by NSF (ASC-9109001) and ONR (N00014-92-J-1686). We also acknowledge the use of computing resources provided by the Ohio Supercomputer Center. M.A.N. was supported by Florida State University through the Supercomputer Computations Research Institute which is partially funded by Department of Energy Contract No. DE-FC05-85ER25000.

¹P. W. Anderson, in *Lectures on the Many Body Problem*, edited by E. R. Caianello (Academic, New York, 1964), Vol. 2, p. 127.

²B. Abeles, *Phys. Rev. B* **15**, 2828 (1977).

³E. Simanek, *Solid State Commun.* **31**, 419 (1979).

⁴L. Jacobs, J. V. Jose, and M. A. Novotny, *Phys. Rev. Lett.* **53**, 2177 (1984).

⁵L. Jacobs, J. V. Jose, M. A. Novotny, and A. Goldman, *Europhys. Lett.* **3**, 1295 (1987).

⁶L. Jacobs, J. V. Jose, M. A. Novotny, and A. Goldman, *Phys. Rev. B* **38**, 4562 (1988).

⁷S. Duane, *Nucl. Phys.* **B257**, 652 (1985); S. Duane and J. B. Kogut, *ibid.* **B275**, 398 (1986).

⁸S. Duane, A. D. Kennedy, B. J. Pendleton, and D. Roweth, *Phys.*

Lett. B **195**, 216 (1986).

⁹J. E. Gubernatis, D. K. Campbell, and X. Wang, in *Computational Approaches in Condensed Matter Physics*, edited by S. Miyashita, M. Imada, and H. Takayama (Springer-Verlag, Berlin, 1992), p. 162; X. Wang, D. K. Campbell, and J. E. Gubernatis (unpublished).

¹⁰W. F. Ames, *Numerical Methods for Partial Differential Equations*, 2nd ed. (Academic, New York, 1964).

¹¹E. Granato, J. M. Kosterlitz, J. Lee, and M. P. Nightingale, *Phys. Rev. Lett.* **66**, 1090 (1991); J. Lee, J. M. Kosterlitz, and E. Granato, *Phys. Rev. B* **43**, 11 531 (1991); J. Lee, E. Granato, and J. M. Kosterlitz, *ibid.* **44**, 4819 (1991).

¹²J. R. Lee (unpublished).